JOURNAL OF THERMOPHYSICS AND HEAT TRANSFER
Vol. 16, No. 3, July–September 2002

Transient Coupled Heat Transfer in Three-Layer Composite with Opaque Specular Surfaces

Jian-Feng Luo,* Xin-Lin Xia,† and He-Ping Tan‡
Harbin Institute of Technology, 150001 Harbin, People's Republic of China
and
Timothy W. Tong§
Colorado State University, Fort Collins, Colorado 80523-1374

A ray tracing/node analyzing method is applied to investigate one-dimensional transient coupled radiative and conductive heat transfer in a three-layer absorbing and isotropically scattering composite with opaque specular surfaces and semitransparent specular interfaces. The reflectivities of the semitransparent interfaces are angularly dependent and determined by Fresnel's reflective law and Snell's refractive law. The radiative transfer coefficients for calculating the radiative heat source term are deduced by the ray tracing method in combination with the zonal method. The transient energy equation is solved by the fully implicit control-volume method in combination with the spectral band model. The effects of surface emissivity, scattering albedo, refractive index and extinction coefficient on transient coupled heat transfer are investigated in detail under radiative and convective boundary conditions.

Nomenclature

A_{k,T_i} = fractional spectral emissive power of spectral band k at nodal temperature T_i, $\int_{\Delta\lambda_k} \frac{I_{\lambda,b}(T_i)\,\mathrm{d}\lambda}{\sigma T_i^4}$

$a1, a2$ = surface, interface or control volume, used to define one-layer radiative intensity quotient transfer function

$b1, b2$ = surface or interface, used to define two-layer radiative intensity quotient transfer function

c_b = specific heat capacity of bth layer, J kg^{-1} K^{-1}

$\boldsymbol{E}$ = radiative intensity quotient transfer function of two-layer semitransparent medium (STM) model

$\boldsymbol{F}$ = radiative intensity quotient transfer function of one-layer STM model

h_1, h_2 = convective heat-transfer coefficients at surfaces S_1 and S_2, respectively, W m^{-2} K^{-1}

I_b = Ith node in bth layer

k_b = thermal conductivity of bth layer of medium, W m^{-1} K^{-1}

k_{ie}, k_{iw} = harmonic mean thermal conductivity at interface ie and iw, W m^{-1} K^{-1}

L_b = thickness of bth layer, m

L_t = total thickness of composite, $L_1 + L_2 + L_3$, m

M_b = number of control volumes of bth layer

M_t = total number of control volumes of composite, $M_1 + M_2 + M_3$

NB = total number of spectral bands

N_b = conduction-radiationparameter of bth layer of medium, $k_b/(4\sigma T_r^3 L_t)$

$n_{b,k}$ = spectral refractive index of bth layer

$n'_{i,k}$ = refractive index of ith control volume; when $i \le M_1$, $n'_{i,k} = n_{1,k}$; when $M_1 < i \le M_1 + M_2$, $n'_{i,k} = n_{2,k}$; when $M_1 + M_2 < i \le M_t$, $n'_{i,k} = n_{3,k}$

n_0, n_4 = refractive indexes of the surroundings (equal to the refractive index of air n_g; Fig. 1)

P, Q = interfaces in composite (Fig. 1)

P_1, P_2 = sides of interface P facing toward the first and the second layers, respectively

Q_2, Q_3 = sides of interface Q facing toward the second and the third layers, respectively

q^c, q^r = thermal conductive and radiative heat fluxes, respectively, W m^{-2}

q^t = total heat flux, $q^c + q^r$, W m^{-2}

$\tilde{q}$ = dimensionless heat flux, $q/(\sigma T_r^4)$

S_u, S_v = surfaces, $u, v = 1$ or 2

$(S_u S_v)_k, [S_u S_v]_k$ = ratios of radiative energy arriving at S_v to that emitted from S_u in the kth spectral band ($\Delta\lambda_k$) for nonscattering and scattering media, respectively

$(S_u V_j)_k, [S_u V_j]_k$ = ratios of radiative energy arriving at V_j to that emitted from S_u in the kth spectral band ($\Delta\lambda_k$) for nonscattering and scattering media, respectively

S_1, S_2 = boundary surfaces (Fig. 1)

$S_{-\infty}, S_{+\infty}$ = left and right black surfaces representing the surroundings (Fig. 1)

T = absolute temperature, K

T_{g1}, T_{g2} = gas temperatures for convection at $x = 0$ and L_t, respectively, K

T_r = reference temperature, K

T_{S_1}, T_{S_2} = temperatures of the boundary surfaces S_1 and S_2, respectively, K

Received 30 October 2000; revision received 13 December 2001; accepted for publication 15 December 2001.

*Ph.D. Candidate, School of Energy Science and Engineering, 92 West Dazhi Street; luo_jianfeng@yahoo.com.

†Associate Professor, School of Energy Science and Engineering, 92 West Dazhi Street.

‡Professor, School of Energy Science and Engineering, 92 West Dazhi Street; tanhp77@hotmail.com.

§Professor, Department of Mechanical Engineering. Associate Fellow AIAA.

T_0 = uniform initial temperature, K
$T_{-\infty}$, $T_{+\infty}$ = temperatures of the black surface $S_{-\infty}$ and $S_{+\infty}$, respectively, K (Fig. 1)
t = physical time, s
V_{I_b} = Ith control volume of bth layer, $I = 1 \sim M_b$
V_i = ith control volume, $i = 1 \sim M_t$
$(V_i S_v)_k$, $[V_i S_v]_k$ = ratios of radiative energy arriving at S_v to that emitted from V_i in the kth spectral band ($\Delta\lambda_k$) for nonscattering and scattering media, respectively
$(V_i V_j)_k$, $[V_i V_j]_k$ = ratios of radiative energy arriving at V_j to that emitted from V_i in the kth spectral band ($\Delta\lambda_k$) for nonscattering and scattering media, respectively
X = dimensionless coordinate in direction across layer, $X = x/L_t$
x = coordinate in direction across layer, m
x_a^b = distance between surface a and b, m
x_i, y_i = geometrical progressions used in tracing radiative intensity's propagation through transmission and reflection
$\alpha_{b,k}$ = spectral absorption coefficient of bth layer, m^{-1}
Γ = attenuated quotient of radiative intensity by control volume or surface [Eq. (5)]
$\gamma(\theta)_{bo}$ = transmissivity of radiative intensity propagating from layer b to layer o at angle θ, $1 - \rho(\theta)_{bo}$
Δt = time interval, s
Δx_b = control volume thickness of bth layer, m
$(\delta x)_{ie}$, $(\delta x)_{iw}$ = distance between nodes i and $i+1$, and that between nodes i and $i-1$, respectively, m (Fig. 1)
$\varepsilon_{0,k}$, $\varepsilon_{1,k}$ = emissivities of the outside and inside of surface S_1, respectively
$\varepsilon_{2,k}$, $\varepsilon_{3,k}$ = emissivities of the inside and outside of surface S_2, respectively
η_b = $1 - \omega_b$
η_i' = $1 - \omega_i'$
Θ = dimensionless temperature, T/T_r
θ = incidence angle
θ_{ij} = critical angle, $\arcsin(n_j/n_i)$, if $n_i > n_j$
$\kappa_{b,k}$ = extinction coefficient of bth layer, $\alpha_{b,k} + \sigma_{s,b,k}$, m^{-1}
λ = wavelength, μm
μ = $\cos\theta$
ρ_b = density of bth layer of medium, kg m^{-3}
$\rho(\theta)_{bo}$ = reflectivity of intensity going from layer b to layer o at angle θ
σ = Stefan–Boltzmann constant, W m^{-2} K^{-4}
$\sigma_{s,b,k}$ = spectral scattering coefficient of bth layer, m^{-1}
Φ_i^r = radiative heat source term of control volume i
$\omega_{b,k}$ = spectral scattering albedo of bth layer, $\sigma_{s,b,k}/\kappa_{b,k}$
$\omega_{i,k}'$ = spectral scattering albedo of ith control volume; when $i \le M_1$, $\omega_{i,k}' = \omega_{1,k}$; when $M_1 < i \le M_1 + M_2$, $\omega_{i,k}' = \omega_{2,k}$; when $M_1 + M_2 < i \le M_t$, $\omega_{i,k}' = \omega_{3,k}$

Subscripts

b = layer index: $b = 1, 2, 3$
bo = intensity propagating from layer b to layer o
c = cth layer, either b or o layer
g = gas (air)
i, j = relative to nodes; index of geometrical progression term
iw, ie = left and right interfaces of ith control volume
k = relative to kth spectral band
o = oth layer, either $b-1$ or $b+1$ layer
o–o = refers to a composite with opaque surfaces
S_1, S_2 = relative to S_1 and S_2
u, v = 1 or 2, relative to S_1 and S_2
$-\infty$, $+\infty$ = relative to $S_{-\infty}$ and $S_{+\infty}$
//, $\perp$ = relative to component for parallel and perpendicular polarization, respectively

Superscripts

c = conduction
m = time step
r = radiation
s = specular reflection
t = total heat flux
$*$ = normalized values

Introduction

TRANSIENT coupled radiative-conductive heat transfer in semitransparent media (STM) is pervasive in engineering applications, such as the processing of glass products[1] and insulating techniques for the protection of aeroengines.[2,3] In this paper transient coupled radiative-conductive heat transfer in a three-layer absorbing isotropically scattering composite medium with opaque specular surfaces and semitransparent specular interfaces is analyzed.

Coupled heat transfer in a single semitransparent layer with specular surfaces has been investigated by Siewert,[4] Frankel,[5] Ganapol,[6] Schwander et al.,[7] Su and Sutton,[8] and Abulwafa et al.[9] A two-layer semitransparent composite with semitransparent surfaces and interfaces has been investigated by Tan et al.,[10] and the effects of both specular and diffuse reflection on coupled heat transfer are discussed. But for a three-layer composite, reflection and total reflection become much more complex than that for a two-layer composite, and the tracing method, used in Ref. 10, is not fit for this condition. So one-layer and two-layer radiative intensity transfer models, as shown in the Appendix, are put forward here to improve the tracing method.

For specular reflection, if the interface is semitransparent reflectivity at the interface is angularly dependent and determined by the Fresnel reflectivity coupled with Snell's law.[6–11] For coupled radiative-conductive heat transfer in a multilayer composite with semitransparent and specular interfaces, the arrangement of refractive index is arbitrary. So reflection, especially total reflection, is very complex. This problem is solved by the ray tracing method in combination with Hottel and Sarofim's zonal method[12] in this paper.

In Ref. 11 Siegel divided the unpolarized radiative incidence into two equal, parallel and perpendicular, components and then traced them separately. Corresponding to these two components, the specular reflectivity at an interface is classified as parallel and perpendicular, as shown in the Appendix. This method of dealing with unpolarized radiative incidence is adopted in this paper.

Physical Model and Governing Equation

Physical Model

As shown in Fig. 1, a three-layer composite of absorbing and isotropically scattering STM is located between two black surfaces $S_{-\infty}$ and $S_{+\infty}$, which respectively denote the surroundings outside the two opaque specular boundary surfaces S_1 and S_2. The interfaces P and Q are semitransparent and specular. The optical and thermal properties of the medium in each layer are different from those of the other layers.

The three layers are divided into M_1, M_2, and M_3, control volumes, respectively, and I_1, I_2, and I_3 are used to denote the Ith nodes in the first, second, and third layers, respectively. Let $M_t = M_1 + M_2 + M_3$. Then the total node number is $M_t + 2$ $(0, 1, \ldots, M_t + 1)$ with node 0 locating S_1 and node $M_t + 1$ locating S_2. For convenience, all of the nodes are denoted by i except for the radiative transfer coefficient (RTC) expressions. The variation of the spectral

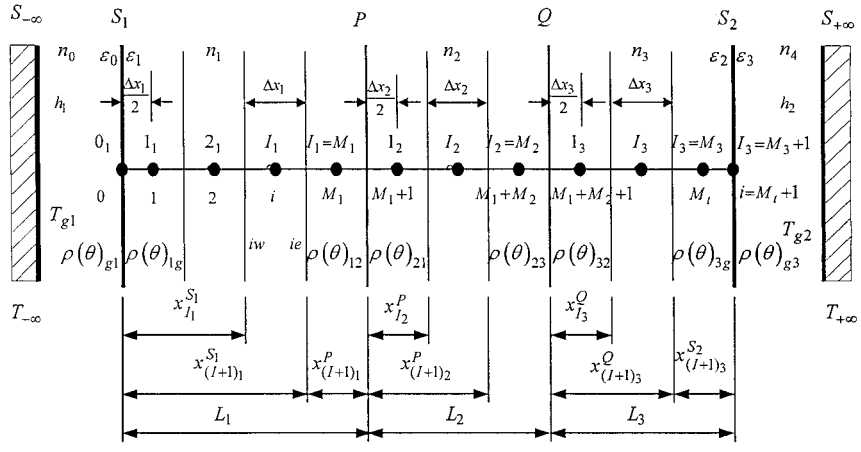

Fig. 1 Physical model of a three-layer semitransparent composite.

parameters, such as κ_b, α_b, $\sigma_{s,b}$, and n_b, with respect to wavelength are expressed by a series of rectangular spectral bands.[10]

Discrete Governing Equation and Boundary Conditions

The fully implicit discrete energy equation of the ith control volume in the bth layer is[10]

$$\rho_b c_b \Delta x_b \frac{T_i^{m+1} - T_i^m}{\Delta t} = \frac{k_{\text{ie}}^{m+1}\left(T_{i+1}^{m+1} - T_i^{m+1}\right)}{(\delta x)_{\text{ie}}} - \frac{k_{\text{iw}}^{m+1}\left(T_i^{m+1} - T_{i-1}^{m+1}\right)}{(\delta x)_{\text{iw}}} + \Phi_i^{r,m+1} \tag{1}$$

Equation (1) is the same with that used in Ref. 10 except for $(\delta x)_{\text{ie}}$ and $(\delta x)_{\text{iw}}$, with mean variable grid size in each layer. By referring to the expression for the radiative source term of the two-layer composite in Ref. 10, the radiative heat source term Φ_i^r of the three-layer composite can be written as $\Phi_i^r = q_{\text{iw}}^r - q_{\text{ie}}^r = q_{(i-1)e}^r - q_{\text{ie}}^r$, where q_{ie}^r is[10]

$$\begin{aligned} q_{\text{ie}}^r = \sigma \sum_{k=1}^{NB} \Bigg[\sum_{j=i+1}^{M_t} \Big(& n_{1,k}'^2 [S_1 V_j]_{k,o-o}^s A_{k,T_{S_1}} T_{S_1}^4 \\ & - n_{j,k}'^2 [V_j S_1]_{k,o-o}^s A_{k,T_j} T_j^4 \Big) + \sum_{l=1}^{i} \sum_{j=i+1}^{M_t} \Big(n_{l,k}'^2 [V_l V_j]_{k,o-o}^s A_{k,T_l} T_l^4 \\ & - n_{j,k}'^2 [V_j V_l]_{k,o-o}^s A_{k,T_j} T_j^4 \Big) + \sum_{l=1}^{i} \Big(n_{l,k}'^2 [V_l S_2]_{k,o-o}^s A_{k,T_l} T_l^4 \\ & - n_{M_t,k}'^2 [S_2 V_l]_{k,o-o}^s A_{k,T_{S_2}} T_2^4 \Big) + n_{1,k}'^2 [S_1 S_2]_{k,o-o}^s A_{k,T_{S_1}} T_{S_1}^4 \\ & - n_{M_t,k}'^2 [S_2 S_1]_{k,o-o}^s A_{k,T_{S_2}} T_{S_2}^4 \Bigg] \qquad 1 \le i < M_t \end{aligned} \tag{2}$$

The sum of radiation and conduction to surface S_1 from inside the composite medium is equal to the sum of radiation and convection leaving the outside of surface S_1, that is,

$$\begin{aligned} \sigma \sum_{k=1}^{NB} \Bigg[& \sum_{j=1}^{M_t} \Big(n_{j,k}'^2 [V_j S_1]_{k,o-o}^s A_{k,T_j} T_j^4 - n_{1,k}'^2 [S_1 V_j]_{k,o-o}^s A_{k,T_{S_1}} T_{S_1}^4 \Big) \\ & + n_{M_t,k}'^2 [S_2 S_1]_{k,o-o}^s A_{k,T_{S_2}} T_{S_2}^4 - n_{1,k}'^2 [S_1 S_2]_{k,o-o}^s A_{k,T_{S_1}} T_{S_1}^4 \Bigg] \\ & + \frac{2k_1\left(T_1 - T_{S_1}\right)}{\Delta x_1} = \sigma \sum_{k=1}^{NB} n_0^2 \varepsilon_{0,k} \left(A_{k,T_{S_1}} T_{S_1}^4 - A_{k,T_{-\infty}} T_{-\infty}^4 \right) \\ & + h_1\left(T_{S_1} - T_{g1}\right) \end{aligned} \tag{3}$$

The discrete boundary condition of surface S_2 is similar to Eq. (3).

RTCs for a Three-Layer Semitransparent Composite

The RTC of element (surface or control volume) i to element j is defined as the quotient of the radiative energy that is received by element j to that emitted by element i. The radiation transfer process in scattering STM can be divided into two subprocesses[13]: 1) emitting-attenuating-reflecting subprocess and 2) absorbing-scattering subprocess.

In the first subprocess only the attenuation and emission of medium are considered. For this condition the RTCs are represented by $(S_u S_v)_{k,o-o}^s$, $(S_u V_i)_{k,o-o}^s$, $(V_i S_u)_{k,o-o}^s$, and $(V_i V_j)_{k,o-o}^s$. In the second subprocess scattering is considered, and then the radiative energy represented by the RTCs $(V_i V_j)_{k,o-o}^s$ etc. is redistributed. For isotropic scattering the radiative energy scattered by element j is uniformly distributed, and such a distribution is treated as being equivalent to emission by element j. When the effect of isotropic scattering is considered, the RTCs are represented by $[S_u S_v]_{k,o-o}^s$, $[S_u V_i]_{k,o-o}^s$, $[V_i S_u]_{k,o-o}^s$, and $[V_i V_j]_{k,o-o}^s$.

RTCs for Emitting-Attenuating-Reflecting Subprocess

The total $(M_t + 2)^2$ RTCs of the three-layer composite medium can be classified into 25 categories, and, as an example, five pairs of them are listed next:

$$\begin{aligned} n_{1,k}^2 (S_1 S_2)_{k,o-o}^s &= n_{3,k}^2 (S_2 S_1)_{k,o-o}^s \\ n_{2,k}^2 \left(V_{I_2} S_2\right)_{k,o-o}^s &= n_{3,k}^2 \left(S_2 V_{I_2}\right)_{k,o-o}^s \\ n_{1,k}^2 \left(V_{I_1} V_{I_2}\right)_{k,o-o}^s &= n_{2,k}^2 \left(V_{I_2} V_{I_1}\right)_{k,o-o}^s \\ n_{2,k}^2 \left(V_{I_2} V_{I_3}\right)_{k,o-o}^s &= n_{3,k}^2 \left(V_{I_3} V_{I_2}\right)_{k,o-o}^s \\ \left(V_{I_1} V_{J_1}\right)_{k,o-o}^s &= \left(V_{J_1} V_{I_1}\right)_{k,o-o}^s \end{aligned} \tag{4}$$

For specularly reflective interfaces and surfaces we can trace a ray to analyze the radiative transfer in the three-layer composite medium. Two basic radiative intensity transfer models of a one-layer medium and a two-layer composite medium, presented in the Appendix, are used in this analysis. The process wherein radiative intensity is attenuated and reflected for so many times that it finally becomes zero is defined as "transferring once," and the symbols $\boldsymbol{F}_{a1_b,k}^{a2_b}$ and $\boldsymbol{E}_{b1_b,b\sim o,k}^{b2_c}$, respectively, represent the radiative intensity quotient transfer functions for these two models, as shown in the Appendix. For example, $\boldsymbol{E}_{P_2,2\sim 3,k}^{P_2}$ denotes the quotient of the kth spectral band radiative intensity finally arriving at P_2 (superscript) to that emitted by P_2 (subscript) after transferring once within the two-layer composite model, which is composed of the second and the third layers (denoted by subscript $2 \sim 3$). The quotient does not indicate that the radiative intensity can pass through interface P and be reflected back through interface P. That is, it only relates to the second and the third layers as well as their interfaces P, Q, and S_2.

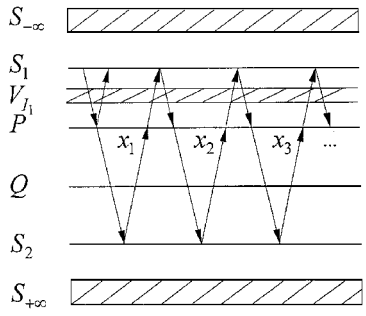

Fig. 2 Sketch of RTC $(S_1V_{I_1})^s_{k,o-o}$ ray trajectories.

Here symbol P_2 denotes the side of interface P facing toward the second layer, whereas the other side of interface P facing toward the first layer is denoted by P_1. A similar definition is applied to interface Q.

The detailed deductive process of RTC $(S_1V_{I_1})^s_{k,o-o}$ is exemplified as follows. For convenience, omit the subscript k in the symbol $\boldsymbol{F}$ and $\boldsymbol{E}$. As shown in Fig. 2, assume S_1 emits a radiative intensity at angle θ, and then we can trace its propagation within the three layers as follows:

1) After the preceding radiative intensity transfers once within the first layer, the portion of it arriving at V_{I_1} for the first time is $y_1 = \boldsymbol{F}_{S_1}^{V_{I_1}}$, and another portion $\boldsymbol{F}_{S_1}^{P_1}\gamma(\theta)_{12}$ of it penetrates into the two-layer composite model, composed of the second and the third layers, through interface P. After transferring once within the two-layer composite model, the portion of the radiative intensity arriving at P_2 for the first time is $x_1 = \boldsymbol{F}_{S_1}^{P_1}\gamma(\theta)_{12}\boldsymbol{E}_{P_2,2\sim3}^{P_2}$ (see Appendix for further explanation).

2) A fraction $\gamma(\theta)_{21}$ of the portion x_1 penetrates into the first layer, and then after transferring once within the first layer the quotient of the radiative intensity received by V_{I_1} to that emitted by S_1 at angle θ for the second time is $y_2 = x_1\gamma(\theta)_{21}\boldsymbol{F}_{P_1}^{V_{I_1}}$, and also a fraction $x_1\gamma(\theta)_{21}\boldsymbol{F}_{P_1}^{P_1}\gamma(\theta)_{12}$ of the radiative intensity penetrates into the two-layer composite again through interface P. Then the quotient of the radiative intensity arriving at P_2 to that emitted by S_1 for the second time, after transferring once within the two-layer composite, is $x_2 = x_1\gamma(\theta)_{21}\boldsymbol{F}_{P_1}^{P_1}\gamma(\theta)_{12}\boldsymbol{E}_{P_2,2\sim3}^{P_2}$.

3) Repeating the tracing process similar to that in step 2 for the fraction x_2, then the quotient of the radiative intensity arriving at V_{I_1} to that emitted by S_1 for the third time is $y_3 = x_2\gamma(\theta)_{21}\boldsymbol{F}_{P_1}^{V_{I_1}}$. Similarly, the nth fraction is $y_n = x_{n-1}\gamma(\theta)_{21}\boldsymbol{F}_{P_1}^{V_{I_1}}$.

The quotients $y_i\,(i \geq 2)$ are an infinite geometric progression with a common ratio of $\beta_2 = \gamma(\theta)_{21}\boldsymbol{F}_{P_1}^{P_1}\gamma(\theta)_{12}\boldsymbol{E}_{P_2,2\sim3}^{P_2}$ (<1). Thus the total quotient of the radiative intensity received by V_{I_1} to that emitted by S_1 at angle θ for each k spectral band is

$$\Gamma = \sum_{i=1}^{\infty} y_i = y_1 + \frac{y_2}{1-\beta_2} = \boldsymbol{F}_{S_1}^{V_{I_1}} + \frac{\boldsymbol{F}_{S_1}^{P_1}\gamma(\theta)_{12}\boldsymbol{E}_{P_2,2\sim3}^{P_2}\gamma(\theta)_{21}\boldsymbol{F}_{P_1}^{V_{I_1}}}{1-\gamma(\theta)_{21}\boldsymbol{F}_{P_1}^{P_1}\gamma(\theta)_{12}\boldsymbol{E}_{P_2,2\sim3}^{P_2}} \tag{5}$$

The transmissivity $\gamma(\theta)$ and reflectivity $\rho(\theta)$ in Eq. (5) are functions of the polarization components, as shown in the Appendix. So corresponding to the parallel and the perpendicular components, the attenuation quotient Γ can be written as $\Gamma_{//}$ and $\Gamma_{\perp}$. Then the total attenuation quotient for the three-layer composite can finally be expressed as $(\Gamma_{//}+\Gamma_{\perp})/2$ for the incidence of unpolarized radiative intensity. By integrating the expression $(\Gamma_{//}+\Gamma_{\perp})/2$ over the hemispherical space and considering the effect of the inside emissivity of S_1 simultaneously, the quotient of the radiative energy received by V_{I_1} to that emitted by S_1 over the hemispherical space $(S_1V_{I_1})^s_{k,o-o}$ can be found. Because of total reflection at interfaces, the integration limits are closely related to the relative magnitudes of the refractive indexes within the composite:

$$\left(S_1V_{I_1}\right)^s_{k,o-o} = \varepsilon_{1,k}\int_0^{\pi/2}(\Gamma_{//}+\Gamma_{\perp})\sin\theta\,\cos\theta\,\mathrm{d}\theta \tag{6}$$

The attenuation quotient Γ is a function to describe the radiative intensity transfer process. Because of total reflection, the values of $\gamma(\theta)$ and $\rho(\theta)$ can change, and Γ is not a continuous function with respect to the variable $\theta \in [0, \pi/2]$. But if a criterion is introduced such as that in the Appendix and the integration range $[0, \pi/2]$ is divided into many intervals according to the values of the critical angles, arranged from small to large, then Γ becomes a continuous function within any of the intervals and applies to any magnitude relationship of the three refractive indexes.

RTCs for Absorbing-Scattering Subprocess

For an absorbing, nonscattering composite the energy represented by the RTCs just deduced is totally absorbed by the second element of each RTC, such as V_{I_1} of $(S_1V_{I_1})^s_{k,o-o}$. But for an absorbing and isotropically scattering composite, part of the energy represented by the RTCs just deduced is absorbed, and the rest is scattered. However, the following process should be further carried out. For convenience, subscript k and superscript s are omitted in the following expressions, and subscript a is introduced to denote the absorption quotient in the deduction. At first, the RTCs calculated for the emitting-attenuating-reflecting subprocess should be normalized:

1) Control volume vs control volume $(V_iV_j)^* = (V_iV_j)/(4\kappa_b\Delta x_b)$, where $V_i \in b$th layer, $i, j = 1 \sim M_t$.

2) Control volume vs surface $(V_iS_u)^* = (V_iS_u)/(4\kappa_b\Delta x_b)$, where $V_i \in b$th layer, $i = 1 \sim M_t$.

3) Surface vs control volume $(S_uV_i)^* = (S_uV_i)/\varepsilon_u$, where $i = 1 \sim M_t$.

4) Surface vs surface $(S_uS_v)^* = (S_uS_v)/(\varepsilon_u)$.

Only the media scatter and the surfaces do not. Take the deductive process for $[S_uV_j]$ as an example:

1) After the first scattering event, part (η'_j) of the fraction of the radiative energy represented by $(S_uV_j)^*$ and absorbed by V_j is $[S_uV_j]^{*1st}_a = (S_uV_j)^*\eta'_j$.

2) The fraction of radiative energy emitted by S_u over the hemispherical space and isotropically scattered by V_{l_2} $(l_2 = 1 \sim M_t)$ is $(S_uV_{l_2})^*\omega'_{l_2}$. This fractional scattered energy can be considered as equivalent to emission by V_{l_2}. So this scattering event causes a part $(S_uV_{l_2})^*\omega'_{l_2}(V_{l_2}V_j)^*\eta'_j$ of the radiative energy to be absorbed by V_j. The total control volume is composed of M_t nodes, and so after the second scattering event the fraction of energy absorbed by V_j becomes

$$[S_uV_j]^{*2nd}_a = [S_uV_j]^{*1st}_a + \sum_{l_2=1}^{M_t}\left(S_uV_{l_2}\right)^*\omega'_{l_2}\left(V_{l_2}V_j\right)^*\eta'_j \tag{7}$$

3) In step 2 a fraction $(S_uV_{l_2})^*\omega'_{l_2}$ of the scattered energy will be scattered again by all of the control volumes, and this causes V_j to absorb some of the radiative energy emitted by S_u for the third scattering event. So after the third scattering event

$$[S_uV_j]^{*3rd}_a = [S_uV_j]^{*2nd}_a + \sum_{l_2=1}^{M_t}\left(S_uV_{l_2}\right)^*\omega'_{l_2}\left[\sum_{l_3=1}^{M_t}\left(V_{l_2}V_{l_3}\right)^*\omega'_{l_3}\left(V_{l_3}V_j\right)^*\eta'_j\right] \tag{8}$$

4) The calculation is finished if $\max\{1-[S_uV_j]^{*nth}_a\} < 10^{-10}$ after the nth scattering event:

$$[S_uV_j]^{*nth}_a = [S_uV_j]^{*(n-1)th}_a + \sum_{l_2=1}^{M_t}\left(S_uV_{l_2}\right)^*\omega'_{l_2}\left[\sum_{l_3=1}^{M_t}\left(V_{l_2}V_{l_3}\right)^*\omega'_{l_3} \times\left(\sum_{l_4=1}^{M_t}\left(V_{l_3}V_{l_4}\right)^*\omega'_{l_4}\cdots\left\{\sum_{l_{n-1}=1}^{M_t}\left(V_{l_{n-2}}V_{l_{n-1}}\right)^*\omega'_{l_{n-1}} \times\left[\sum_{l_n=1}^{M_t}\left(V_{l_{n-1}}V_{l_n}\right)^*\omega'_{l_n}\left(V_{l_n}V_j\right)^*\eta'_j\right]\right\}\right)\right] \tag{9}$$

Then $[S_uV_j]$ can be found from $[S_uV_j] = \varepsilon_u[S_uV_j]^{*nth}_a$. The deductive processes for the rest of the RTCs, such as $[V_iV_j]$,

Table 1 Comparison of the results of this paper with those of Refs. 5 and 13 for transient case

References	Dimensionless temperature, T/T_r			Dimensionless radiative heat flux, $q^r/(k_1\kappa_1 T_r)$		
	$X=\frac{1}{4}$	$X=\frac{1}{2}$	$X=\frac{3}{4}$	$X=0$	$X=\frac{1}{2}$	$X=1$
5: Eighth-order approximation, $\omega=0.5$	0.4893	0.1773	0.0587	1.9342	1.3289	0.8319
13: $\Delta t^*=t^*_{\text{Ref. 5}}/5000$, $M_t=200$, $\omega=0.5$	0.48935	0.17731	0.05869	1.93422	1.32883	0.83190
Current paper: $\Delta t^*=t^*_{\text{Ref. 5}}/1000$, $M_t=397$, $\omega_b=0.5$	0.48924	0.17729	0.05871	1.93425	1.32881	0.83188

$[V_i S_u]$, and $[S_u S_v]$ are similar. Because $\alpha_b=\kappa_b\eta_b$, after the nth scattering event, $[V_i V_j]=4\kappa_b\eta_b\Delta x_b[V_i V_j]_a^{*nth}$ ($V_i\in b$th layer), $[V_i S_u]=4\kappa_b\eta_b\Delta x_b[V_i S_u]_a^{*nth}$, and $[S_u S_v]=\varepsilon_u[S_u S_v]_a^{*nth}$, where the expressions of $[S_u S_v]_a^{*nth}$, $[V_i V_j]_a^{*nth}$, and $[V_i S_u]_a^{*nth}$ are similar to Eq. (9). For simplicity, they are omitted here. By referring to Ref. 13 and Ref. 10, more technical information about the deduction of isotropic scattering RTCs can be found.

Numerical Method and Validation

The radiative heat source term Φ_i^r is a nonlinear function of temperature. It can be linearized by Patankar's method[14,15]:

$$\Phi_i^{r,m,n+1}=\Phi_i^{r,m,n}+\left(\frac{\mathrm{d}\Phi_i^r}{\mathrm{d}T_i}\right)^{m,n}\left(T_i^{m,n+1}-T_i^{m,n}\right)$$
$$=Sc_i^{m,n+1}+Sp_i^{m,n+1}T_i^{m,n+1} \qquad (10)$$

where superscript n and $n+1$ denote the nth and $(n+1)$th iterative calculations; Sc_i represents the constant part of Φ_i^r; Sp_i is the modulus of T_i; and $Sp\le 0$ (Ref. 15). Solving the linearized equations by the tridiagonal matrix algorithm gives the temperatures of all nodes.

The correctness of the RTCs is first validated by Eq. (4) and the following equations:

$$\sum_{j=1}^{M_t}[V_i V_j]^s_{k,o-o}+[V_i S_1]^s_{k,o-o}+[V_i S_2]^s_{k,o-o}$$
$$=4\kappa_b\eta_b\Delta x_b=4\alpha_b\Delta x_b,\qquad V_i\in b\text{th layer}$$

$$\sum_{j=1}^{M_t}[S_u V_j]^s_{k,o-o}+[S_u S_v]^s_{k,o-o}+[S_u S_u]^s_{k,o-o}=\varepsilon_{u,k}$$

$$u,v=1\quad\text{or}\quad 2 \qquad (11)$$

After detailed calculation and careful examination, it is found that Eqs. (4) and (11) are satisfied. For example, for the case of a composite with optical properties of $n_1=1.8$, $n_2=1.5$, $n_3=2$, $\kappa_1=10\ \text{m}^{-1}$, $\kappa_2=100\ \text{m}^{-1}$, $\kappa_3=50\ \text{m}^{-1}$, $\omega_1=\omega_2=\omega_3=0$, and $\varepsilon_1=\varepsilon_2=0.7$; with thickness values of $L_1=L_2=L_3=0.01$ m, we chose the control volumes of this case as $M_1=M_2=M_3=100$. After calculating all of the RTCs, we checked to see if Eqs. (4) and (11) were satisfied. Several pairs of comparison results are listed here:

$$n_{1,k}^2(S_1S_2)^s_{k,o-o}=0.118074314279238$$

$$n_{3,k}^2(S_2S_1)^s_{k,o-o}=0.118074314279368$$

$$n_{2,k}^2\left(V_{90_2}V_{53}\right)^s_{k,o-o}=0.00019439857733$$

$$n_{3,k}^2\left(V_{53}V_{90_2}\right)^s_{k,o-o}=0.00019439857733$$

$$\sum_{j=1}^{M_t}[V_{201}V_j]^s_{k,o-o}+[V_{201}S_1]^s_{k,o-o}+[V_{201}S_2]^s_{k,o-o}$$
$$=0.019999999998,\qquad 4\kappa_3\Delta x_3=0.02$$

$$\sum_{j=1}^{M_t}[S_1V_j]^s_{k,o-o}+[S_1S_2]^s_{k,o-o}+[S_1S_2]^s_{k,o-o}=0.700000000000$$

$$\varepsilon_1=0.7$$

$$\sum_{j=1}^{M_t}[S_2V_j]^s_{k,o-o}+[S_2S_1]^s_{k,o-o}+[S_2S_1]^s_{k,o-o}=0.700000000000$$

$$\varepsilon_2=0.7 \qquad (12)$$

In addition, if the parameters in all layers are allowed to be the same the three-layer composite is equivalent to a one-layer medium. So the results of this investigation can be compared with those of Refs. 5 and 13, which investigated the transient coupled heat transfer in a single layer with opaque surfaces. The parameters used were $\varepsilon_1=\varepsilon_2=1$, $n_1=n_2=n_3=1$, $T_{S_1}=T_r=1000$ K, $T_{S_2}=T_0=0$ K, $\rho_b c_b=\text{constant}$ ($b=1\sim 3$), $\omega_b=0.5$, $N_{b,\text{Ref. 5}}=k_1\kappa_1/(4\sigma T_r^3)=0.1$ (defined by Ref. 5), and $t^*_{\text{Ref. 5}}=k_1\kappa^2 t/(\rho_1 c_1)=0.05$. To let $L_1\kappa_1+L_2\kappa_2+L_3\kappa_3=1$ and for the nodes located at $X=\frac{1}{4}$ and $\frac{3}{4}$ to appear in the calculations, the thickness, extinction coefficient, and control volumes of each layer were chosen as $L_1=L_3=0.1300505$ m, $L_2=0.739899$ m, $\kappa_1=\kappa_2=\kappa_3=1\ \text{m}^{-1}$, $M_1=M_3=52$, $M_2=293$. As shown in Table 1, for the results of $\omega_b=0.5$ good agreement is reached with Refs. 5 and 13.

Results and Discussion

As a special case, a gray medium is analyzed in the following. The parameters for the reference condition are shown in Table 2. By comparing with the reference condition, the effects of surface emissivity, scattering albedo, refractive index, extinction coefficient, and conduction-radiation parameter are investigated.

In the calculations the number of control volumes of each sublayer is chosen as $M_1=M_2=M_3=100$, and a constant time step $\Delta t=t/100$ is applied, which can provide enough precision. The steady state is defined to be reached if $\max|T_i^{m+1}-T_i^m|<10^{-5}$.

Effect of Conduction-Radiation Parameter on Temperature Distribution

Figure 3 shows the effect of changing the conduction-radiation parameters in the three layers as compared to those of the reference condition in Table 2.

With the increase in conduction-radiation parameter, the temperature distribution curves become smoother. For instance, the results for very large conduction-radiation parameters (dashed lines) are almost linear at steady state. The corresponding transient heat-flux distributions are presented in Figs. 4 and 5, respectively. As shown in Fig. 4, the conductive heat fluxes in the first and the second layers are very small. In Fig. 5, however, the increase in the conduction-radiation parameters of the first and the second layers causes the conductive heat fluxes to increase considerably, the radiative heat flux to decrease, and the total heat flux to increase (Table 3). With the evolution of the process, the radiative heat flux in the first layer decreases and that in the third layer increases, but a contrary condition results for the conductive heat flux. When steady state is reached, the total heat flux tends to be a constant value.

Effect of Surface Emissivity on Temperature Distribution

Figure 6 demonstrates surface emissivity effects. As shown by there, an increase in surface emissivity (dashed lines) causes the temperatures in the medium and at the surfaces to increase and the steady heat flux to increase (Table 3). Decreased surface emissivity for S_2 (dash-dot lines) causes the temperatures in the composite medium to increase but the steady heat flux to decrease (Table 3).

Table 2 Reference case parameters

Parameter	Value
$T_{-\infty}$	1000 K
$T_{+\infty}$	500 K
$T_{g1} = T_{g2}$	500 K
T_0	500 K
T_r	1000 K
κ_1	10 m^{-1}
κ_2	100 m^{-1}
κ_3	50 m^{-1}
n_3	2
$h_1 = h_2$	100 W m^{-2} K^{-1}
$\rho_1 c_1$	5×10^4 J m^{-3} K^{-1}
$\rho_2 c_2$	10^5 J m^{-3} K^{-1}
$\rho_3 c_3$	10^4 J m^{-3} K^{-1}
$\varepsilon_0 = \varepsilon_1 = \varepsilon_2 = \varepsilon_3$	0.7
N_1	0.001
N_2	0.006
N_3	0.06
$L_1 = L_2 = L_3$	0.01 m
$\omega_1 = \omega_2 = \omega_3$	0

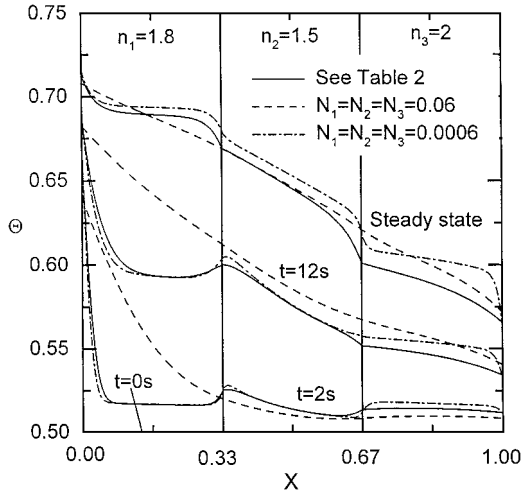

Fig. 3 Effect of conduction-radiation parameter on temperature distribution.

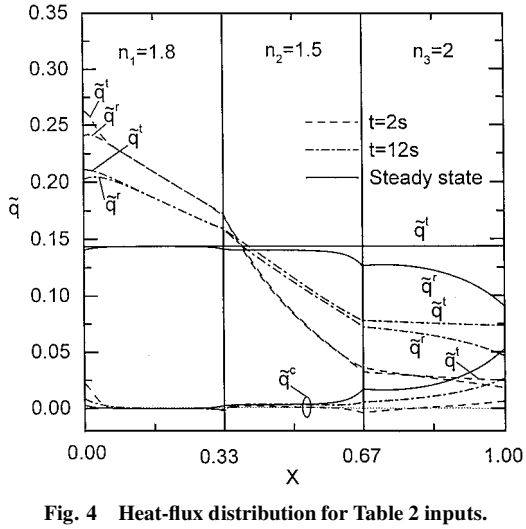

Fig. 4 Heat-flux distribution for Table 2 inputs.

Table 3 Total dimensionless steady-state heat flux ($\tilde{q}^t$)

Line type	Fig. 3	Fig. 6	Fig. 7	Fig. 8	Fig. 9
Solid	0.1436	0.1436	0.1436	0.1436	0.1436
Dashed	0.1578	0.2300	0.1415	0.1215	0.1219
Dash–dot	0.1359	0.1346	0.1389	0.1113	0.1242
Dotted	——	——	——	0.1290	0.1360

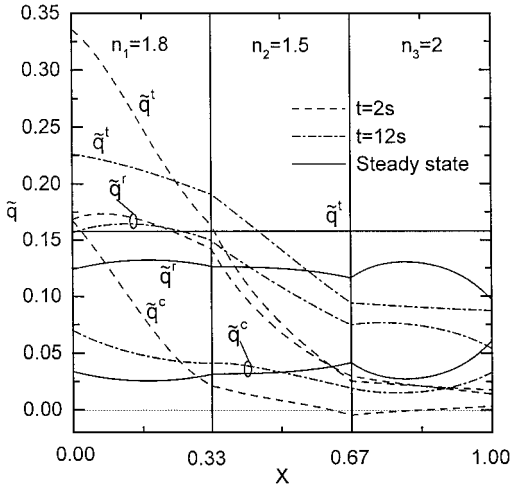

Fig. 5 Heat-flux distribution for $N_1 = N_2 = N_3 = 0.06$.

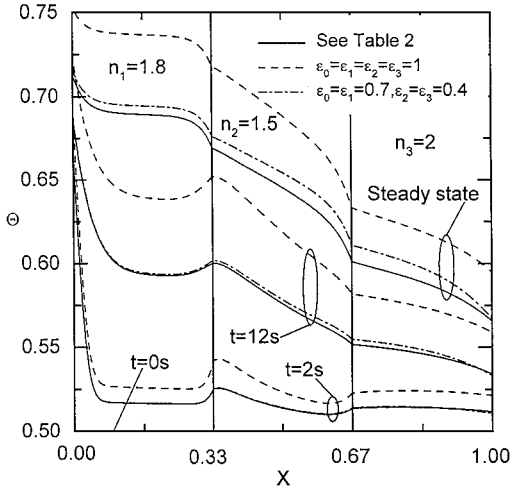

Fig. 6 Effect of surface emissivity on temperature distribution.

The reason is that more radiative energy emitted from S_1 and the medium is reflected back by S_2, and the radiating ability of S_2 to $S_{+\infty}$ for cooling is weakened.

Effect of Scattering Albedo on Temperature Distribution

The increase in scattering albedo causes the emitting-absorbing ability of the composite medium to decrease. So the energy absorbed by S_1 from $S_{-\infty}$ is less adequately reemitted out by S_1 toward the inside of the composite than the reference case does, and at the same time more of the radiative energy, emitted by S_1, is scattered by the composite medium to cause S_2 to absorb more energy. As shown in Fig. 7, compared with the reference case, an increase in scattering albedo causes the surface temperatures to rise fast, the medium temperature in central region of the composite to rise slowly, and the steady state heat flux to decrease.

Effect of Refractive Index on Temperature Distribution

From Fig. 8, when n_1 decreases (dashed lines), the emitting ability of the inside of S_1 is weakened, and so only the temperatures of

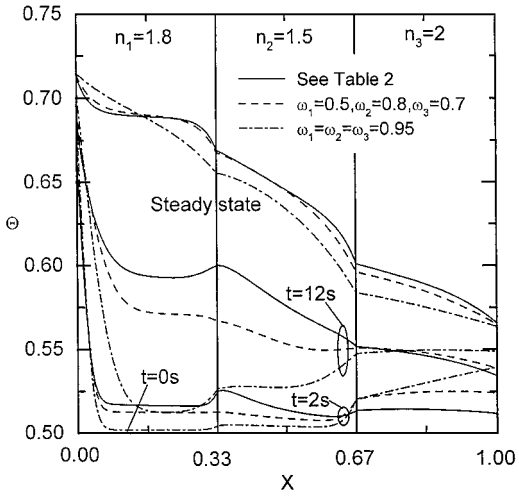

Fig. 7 Effect of scattering albedo on temperature distribution.

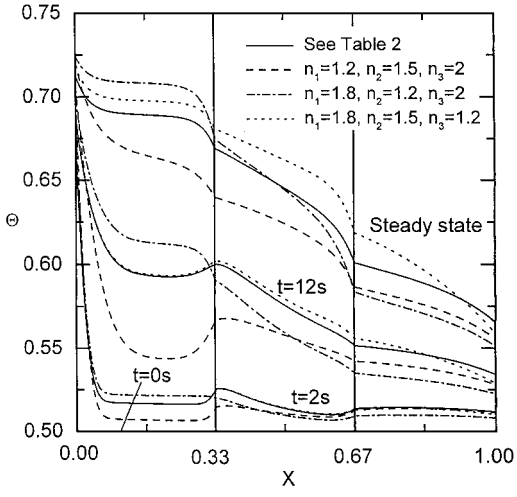

Fig. 8 Effect of refractive index on temperature distribution.

S_1 and its adjacent medium are higher than that of the reference case, but the medium temperature in the main region of the composite is lower. The decrease in n_2 (dash–dot lines), which intensifies reflection and total reflection at interface P, causes more of the radiative energy, emitted by S_1 and the first layer medium, to be reflected back to the first layer at interface P, and so the temperature in the first layer increases and that in the third layer decreases. When n_3 decreases (dotted lines), more of the radiative energy, mainly emitted by S_1, is reflected back to the second and the first layers by interface Q because total reflection is changed from the third layer to the second layer at interface Q, and so the temperature in the main region of the composite increases except for that at surface S_2 and its adjacent region. In addition, the decrease in any of the three refractive indexes can result in a decrease in the steady state heat flux, as shown in Table 3, and so this indicates the heat-transfer ability of the composite is weakened if any of the three refractive indexes decreases. The relative magnitudes of n_1, n_2, and n_3 affect the temperature distribution in the composite medium.

Effect of Extinction Coefficient on Temperature Distribution

As shown in Fig. 9, when the extinction coefficient of the first layer increases (dashed lines) the first layer absorbs more radiative energy emitted by S_1, and less can be transferred into the second and the third layers. So in the transient beginning the temperatures in the second and the third layers decrease and that of the first layer increases. In the steady state the temperatures of most region of the composite decrease except for that of surface S_1 and its adjacent region.

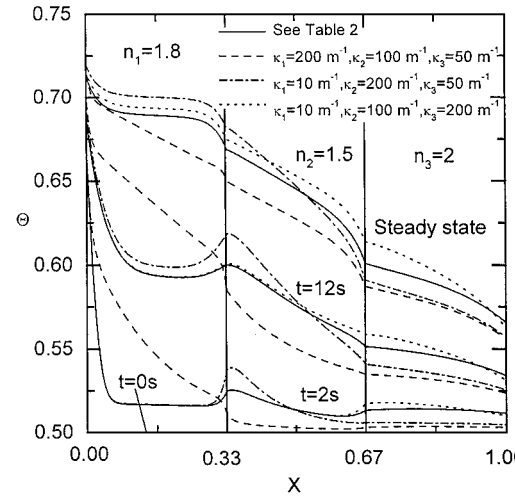

Fig. 9 Effect of extinction coefficient on temperature distribution.

When the extinction coefficient of the second layer increases (dash–dot lines), the second layer intensively absorbs radiative energy coming from its left direction, and so the peak temperature near interface P becomes very clear in this layer, and at the same time the temperature of the third layer falls. In addition the second layer can emit more radiative energy to the first layer because of its intensified emitting ability and causes the temperature of the first layer to rise.

An increase in the extinction coefficient of the third layer (dotted lines) causes the temperatures of the first and the second layers to increase and the temperatures of S_2 and its adjacent region to decrease because of the intensified emitting and absorbing ability of the third layer. As shown in Table 3, an increase in extinction coefficient of any layer will cause the steady-state heat flux to decrease.

Conclusions

By employing the ray-tracing method in combination with Hottel and Sarofim's zonal method, the RTCs for a three-layer absorbing and isotropically scattering composite medium are derived. Using the RTCs, the radiative heat source term in the energy equation is calculated. The transient energy equation is solved by the fully implicit control-volume method in combination with a spectral band model. With combined convection and radiation boundary conditions the transient temperature distribution and heat flux in the composite medium are obtained.

The effects of conduction-radiation parameter, surface emissivity, scattering albedo, refractive index, and extinction coefficient on transient coupled heat transfer are investigated in detail. By comparison and validation the method and results presented in this paper possess the satisfied precision. The following conclusions are made:

1) On the basis of one-layer and two-layer radiative intensity transfer models, a multilayer radiative intensity transfer model can be easily established.

2) For specular and semitransparent interfaces, by introducing a criterion to divide the integration range $[0, \pi/2]$ into many intervals and arranging them according to the values of critical angle the total attenuation quotient Γ can become a continuous function within any of the intervals and fits for any relative magnitude of refractive indexes within the layers.

3) An increase in a layer's conduction-radiation parameter or in surface emissivity tends to make the steady-state heat flux increase.

4) With constant extinction coefficient an increase in scattering albedo of a layer causes the steady-state heat flux to decrease.

5) A decrease in refractive index or an increase in the extinction coefficient of any layer will weaken the heat transfer in the composite medium. The relative magnitudes of the refractive indexes and the extinction coefficients in the three layers affect the temperature distribution.

Appendix: Two Basic Radiative Intensity Transfer Models

For semitransparent composite with specular and semitransparent interfaces, we can trace a ray emitted at an arbitrary angle to get the attenuation expression. Two basic radiative intensity transfer models for a one-layer medium and a two-layer composite medium are put forward here, which are very helpful to derive the RTCs for a three-layer composite. The symbols $\boldsymbol{F}^{a2_b}_{a1_b,k}$ and $\boldsymbol{E}^{b2_c}_{b1_b,b\sim o,k}$ are introduced respectively to represent the radiative intensity quotient transfer functions for the two models, which mean the ratios of the spectral radiative intensity arriving at $a2_b$ (superscript) (or $b2_c$) to that emitted by $a1_b$ (subscript) (or $b1_b$) in the kth spectral band. Symbols b, c, and o denote the bth, cth, and oth layers, respectively, and $o=b-1$ or $b+1$, $c=b$ or o. Subscript $b\sim o$ denotes that the two-layer composite medium is composed of the bth and its adjoining oth layers.

In allusion to the deductive process for determining $(S_1 V_{I_1})^s_{k,o-o}$, a detailed description of the basic radiative intensity transfer models is presented as follows. For convenience, the subscript k is omitted here.

One-Layer Basic Radiative Intensity Transfer Model

Assume that the two parallel boundaries of the bth layer are A and B. Radiative intensity, emitted by the mth element (surface or control volume) in the θ direction, enters the bth layer through boundary A or B. Then the radiative intensity will be attenuated and reflected repeatedly within the layer until it finally becomes 0. By tracing the transfer process, the following expressions are obtained:

$$\boldsymbol{F}^{V_{I_b}}_{A_b} = \Big(\rho(\theta)_{b,b+1}\exp\big\{-\kappa_b\big[L_b + x^{B_b}_{(I+1)_b}\big]\big/\mu_b\big\} + \exp\big(-\kappa_b x^{A_b}_{I_b}\big/\mu_b\big)\Big)[1-\exp(-\kappa_b\Delta x_b/\mu_b)]/(1-\beta_1)$$

$$\boldsymbol{F}^{V_{I_b}}_{B_b} = \big\{\rho(\theta)_{b,b-1}\exp\big[-\kappa_b\big(L_b + x^{A_b}_{I_b}\big)\big/\mu_b\big] + \exp\big[-\kappa_b x^{B_b}_{(I+1)_b}\big/\mu_b\big]\big\}[1-\exp(-\kappa_b\Delta x_b/\mu_b)]/(1-\beta_1)$$

$$\boldsymbol{F}^{B_b}_{B_b} = \exp(-2\kappa_b L_b/\mu_b)\rho(\theta)_{b,b-1}/(1-\beta_1)$$

$$\boldsymbol{F}^{A_b}_{A_b} = \exp(-2\kappa_b L_b/\mu_b)\rho(\theta)_{b,b+1}/(1-\beta_1) \tag{A1}$$

where $\beta_1 = \exp(-2\kappa_b L_b/\mu_b)\rho(\theta)_{b,b-1}\rho(\theta)_{b,b+1}$, $\mu_b = \cos\theta_b$, and θ_b is the propagation angle in the bth layer. According to Snell law, the relationship between θ and θ_b is[16]

$$\theta_b = \arcsin(n_m \sin\theta/n_b) \tag{A2}$$

The detailed form of Eq. (A1) for each layer of the three-layer composite is obtained if the following replacements are made: 1) for the first layer $b=1$, $A=S$, and $B=P$; 2) for the second layer $b=2$, $A=P$, and $B=Q$; 3) for the third layer $b=3$, $A=Q$, and $B=S$.

The reflectivity $\rho(\theta)$ in Eq. (A1) is a function of polarization component, and so the form of each function $\boldsymbol{F}^{a2_b}_{a1_b}$ in Eq. (A1) corresponds to the perpendicular and parallel components. For a perfect dielectric medium the effect of the extinction coefficient in the complex index of refraction can be neglected. When radiative intensity enters the adjoining oth layer from the bth layer at angle θ_b, the reflectivity $\rho(\theta_b)_{\rm bo}$ is[11,16]

$$\rho_{//}(\theta_b)_{\rm bo} = \left[\frac{\tan(\theta_b-\varphi_o)}{\tan(\theta_b+\varphi_o)}\right]^2 \quad \text{(for parallel component)} \tag{A3a}$$

$$\rho_{\perp}(\theta_b)_{\rm bo} = \left[\frac{\sin(\theta_b-\varphi_o)}{\sin(\theta_b+\varphi_o)}\right]^2 \quad \text{(for perpendicular component)} \tag{A3b}$$

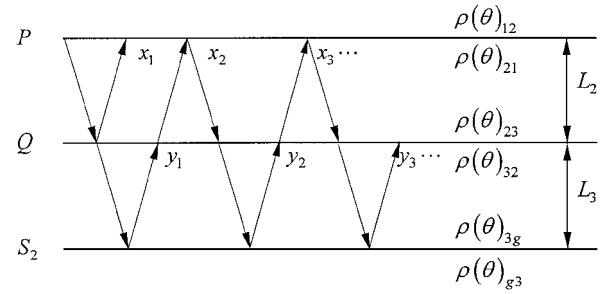

Fig. A1 Two-layer basic radiative intensity transfer model.

where φ_o is the propagation angle in the oth layer. According to Snell's refractive law,[16]

$$\varphi_o = \arcsin(n_b \sin\theta_b/n_o) \tag{A4}$$

Substituting Eq. (A2) into Eqs. (A3) and (A4), the reflectivity $\rho(\theta_b)_{\rm bo}$ can be written as $\rho(\theta)_{\rm bo}$, which becomes a function of angle θ. So, if any element (surface or control volume) emits radiative intensity at an angle θ the specular reflectivities at all interfaces for the radiative intensity propagating within the three-layer composite are determined by θ. When $n_b > n_o$ and if $\theta_b > \arcsin(n_o/n_b)$, total reflection occurs, and $\rho(\theta)_{\rm bo}=1$. When radiative intensity propagates in the reverse direction, the reflectivity is $\rho(\theta)_{\rm ob}=\rho(\theta)_{\rm bo}$, if total reflection $\rho(\theta)_{\rm ob}=1$ does not occur. If $n_b=n_o$, then $\rho(\theta)_{\rm ob}=\rho(\theta)_{\rm bo}=0$.

If the boundary is opaque, such as S_1 and S_2, then the reflectivity is $\rho(\theta)=1-\varepsilon$, where, ε is the emissivity of the opaque surface.

Two-Layer Basic Radiative Intensity Transfer Model

Based on the one-layer basic radiative intensity transfer model, the two-layer model can be created. Taking $\boldsymbol{E}^{P_2}_{P_2,2\sim 3}$ as an example, as shown in Fig. A1, the detailed deduction of the two-layer radiative intensity quotient transfer function is presented next:

1) Assuming P_2 emits radiative intensity, then after transferring once in the second layer the quotient of the radiative intensity arriving at P_2 for the first time is $x_1=\boldsymbol{F}^{P_2}_{P_2}$, and a fraction $\boldsymbol{F}^{Q_2}_{P_2}\gamma(\theta)_{23}$ of the radiative intensity enters the third layer through the interface Q. Then after transferring once in the third layer the quotient of the radiative intensity arriving at Q_3 for the first time is $y_1=\boldsymbol{F}^{Q_2}_{P_2}\gamma(\theta)_{23}\boldsymbol{F}^{Q_3}_{Q_3}$.

2) Next, a fraction $\gamma(\theta)_{32}$ of the quotient y_1 enters the second layer. Then after transferring once in the second layer the quotient of the radiative intensity arriving at P_2 for the second time is $x_2=y_1\gamma(\theta)_{32}\boldsymbol{F}^{P_2}_{Q_2}$. Again, a fraction $y_1\gamma(\theta)_{32}\boldsymbol{F}^{Q_2}_{Q_2}\gamma(\theta)_{23}$ of the radiative intensity enters the third layer, and after transferring once within the third layer the quotient of the radiative intensity arriving at Q_3 for the second time is $y_2=y_1\gamma(\theta)_{32}\boldsymbol{F}^{Q_2}_{Q_2}\gamma(\theta)_{23}\boldsymbol{F}^{Q_3}_{Q_3}$.

3) Repeating step 2 for quotient y_2, then the quotient of the radiative intensity arriving at P_2 for the third time is $x_3=y_2\gamma(\theta)_{32}\boldsymbol{F}^{P_2}_{Q_2}$, and that arriving at Q_3 for the third time is $y_3=y_2\gamma(\theta)_{32}\boldsymbol{F}^{Q_2}_{Q_2}\gamma(\theta)_{23}\boldsymbol{F}^{Q_3}_{Q_3}$.

Trace the transfer process in this way until the radiative intensity finally attenuates to 0. Here, $x_i (i\geq 2)$ is an infinite geometric series with a common ratio of $\beta_2=\gamma(\theta)_{32}\boldsymbol{F}^{Q_2}_{Q_2}\gamma(\theta)_{23}\boldsymbol{F}^{Q_3}_{Q_3}$ (and $\beta_2<1$). Then the total quotient of the intensity emitted by P_2 and finally arriving at P_2 is derived as

$$\boldsymbol{E}^{P_2}_{P_2,2\sim 3} = x_1 + \sum_{i=2}^{\infty} x_i = \boldsymbol{F}^{P_2}_{P_2} + \frac{\boldsymbol{F}^{Q_2}_{P_2}\gamma(\theta)_{23}\boldsymbol{F}^{Q_3}_{Q_3}\gamma(\theta)_{32}\boldsymbol{F}^{P_2}_{Q_2}}{1-\beta_2} \tag{A5}$$

If all corresponding parameters of the two layers are the same, the two-layer model transforms into a one-layer model with a thickness of $L=L_2+L_3$, and the two-layer radiative intensity quotient transfer function $\boldsymbol{E}^{P_2}_{P_2,2\sim 3}$ can transform into the one-layer radiative intensity quotient transfer function by using the relationship $\rho(\theta)_{23}=\rho(\theta)_{32}=0$, that is, $\boldsymbol{E}^{P_2}_{P_2,2\sim 3}=\boldsymbol{F}^{P_2}_{P_2,2\sim 3}$.

Acknowledgments

This research is supported by the Chinese National Science Fund for Distinguished Young Scholars (59725617), the National Natural Science Foundation of China (50076010), and the Fok Ying Tung Education Foundation (71053). Jian-Feng Luo is very grateful to Ronald L. Dougherty for his guidance and for his important revision on this paper.

References

[1]Ducharme, R., Kapadia, P., Scarfe, F., and Dowden, J., "A Mathematical-Model of Glass Flow and Heat-Transfer in a Platinum Downspout," *International Journal of Heat and Mass Transfer*, Vol. 36, No. 7, 1993, pp. 1789–1797.

[2]Siegel, R., "Temperature Distribution in Channel Walls with Translucent Thermal Barrier Coatings," *Journal of Thermophysics and Heat Transfer*, Vol. 12, No. 3, 1998, pp. 289–296.

[3]Siegel, R., "Green's Function to Determine Temperature Distribution in a Semitransparent Thermal Barrier Coating," *Journal of Thermophysics and Heat Transfer*, Vol. 11, No. 2, 1997, pp. 315–318.

[4]Siewert, C. E., "An Improved Iterative Method for Solving a Class of Coupled Conductive-Radiative Heat Transfer Problems," *Journal of Quantitative Spectroscopy and Radiative Transfer*, Vol. 54, No. 4, 1995, pp. 599–605.

[5]Frankel, J. I., "Cumulative Variable Formulation for Transient Conductive and Radiative Transport in Participating Medium," *Journal of Thermophysics and Heat Transfer*, Vol. 9, No. 2, 1995, pp. 210–218.

[6]Ganapol, B. D., "Radiative Transfer in a Semiinfinite Medium with a Specularly Reflecting Boundary," *Journal of Quantitative Spectroscopy and Radiative Transfer*, Vol. 53, No. 3, 1995, pp. 257–267.

[7]Schwander, D., Flamant, G., and Olalde, G., "Effects of Boundary Properties on Transient Temperature Distributions in Condensed Semitransparent Media," *International Journal of Heat and Mass Transfer*, Vol. 41, No. 14, 1998, pp. 2083–2096.

[8]Su, M. H., and Sutton, W. H., "Transient Conductive and Radiative Heat Transfer in a Silica Window," *Journal of Thermophysics and Heat Transfer*, Vol. 9, No. 2, 1995, pp. 370–373.

[9]Abulwafa, E. M., "Conductive-Radiative Heat Transfer in an Inhomogeneous Slab with Directional Raflecting Boundaries," *Journal of Physics. D: Applied Physics*, Vol. 32, No. 14, 1999, pp. 1626–1632.

[10]Tan, H. P., Wang, P. Y., and Xia, X. L., "Transient Coupled Radiation and Conduction in an Absorbing and Scattering Composite Layer," *Journal of Thermophysics and Heat Transfer*, Vol. 14, No. 1, 2000, pp. 77–87.

[11]Siegel, R., "Effects of Refractive Index and Diffuse or Specular Boundaries on a Radiating Isothermal Layer," *Journal of Heat Transfer*, Vol. 116, No. 3, 1994, pp. 787–790.

[12]Hottel, H. C., and Sarofim, A. F., *Radiative Transfer*, McGraw–Hill, New York, 1967, pp. 265, 266.

[13]Tan, H. P., Ruan, L. M., Xia, X. L., Yu, Q. Z., and Tong, T. W., "Transient Coupled Radiative and Conductive Heat Transfer in an Absorbing, Emitting and Scattering Medium," *International Journal of Heat and Mass Transfer*, Vol. 42, No. 15, 1999, pp. 2967–2980.

[14]Patankar, S. V., *Numerical Heat Transfer and Fluid Flow*, McGraw–Hill, New York, 1980 (Translated by Zhang Zheng, Science Press, Beijing, 1989, pp. 53–56).

[15]Tan, H. P., and Lallemand, M., "Transient Radiative-Conductive Heat Transfer in Flat Glasses Submitted to Temperature, Flux and Mixed Boundary Conditions," *International Journal of Heat and Mass Transfer*, Vol. 32, No. 5, 1989, pp. 795–810.

[16]Siegel, R., and Howell, J. R., *Thermal Radiative Heat Transfer*, McGraw–Hill, New York, 1981, p. 95.